

Optical rotatory power of polymer-stabilized blue phase liquid crystals

Yifan Liu,¹ Yi-fen Lan,^{1,2} Hongxia Zhang,^{1,3} Ruidong Zhu,¹ Daming Xu,¹ Cheng-Yeh Tsai,² Jen-Kuei Lu,² Norio Sugiura,² Yu-Chieh Lin,² and Shin-Tson Wu^{1,a)}

¹College of Optics and Photonics, University of Central Florida, Orlando, Florida 32816, USA

²AU Optonics Corp., Hsinchu Science Park, Hsinchu 300, Taiwan

³Tianjin University, 92 Weijin Road, Nankai District, Tianjin 300072, China

(Received 23 January 2013; accepted 20 March 2013; published online 1 April 2013)

Macroscopically, a polymer-stabilized blue phase liquid crystal (BPLC) is assumed to be an optically isotropic medium. Our experiment challenges this assumption. Our results indicate that the optical rotatory power (ORP) of some nano-scale double-twist cylinders in a BPLC composite causes the polarization axis of the transmitted light to rotate a small angle, which in turn leaks through the crossed polarizers. Rotating the analyzer in azimuthal direction to correct this ORP can greatly improve the contrast ratio. A modified De Vries equation based on a thin twisted-nematic layer is proposed to explain the observed phenomena. © 2013 American Institute of Physics. [<http://dx.doi.org/10.1063/1.4799511>]

A polymer-stabilized blue phase liquid crystal (PS-BPLC) is a self-assembly nanostructure electro-optic medium.¹⁻⁷ The self-assembly process forms three dimensional lattices without the need of surface alignment agent, and the voltage-off state is optically isotropic. The short coherence length leads to submillisecond response time.^{6,7} Thus, BPLC holds potential for high speed display and photonic devices. However, some critical issues, such as relatively high operation voltage, noticeable hysteresis, and limited contrast ratio (CR), remain to be overcome. Several promising approaches for reducing operation voltage⁸⁻¹⁰ and suppressing hysteresis^{11,12} have been demonstrated, but the problem of CR remains unexplored. Most nematic liquid crystal display (LCD) devices can reach CR > 5000:1, but BPLCs can barely reach ~1000:1.^{5,13} The low CR of a PS-BPLC mainly originates from the dark state light leakage. There is an urgent need to understand the light leakage mechanism and then improve the contrast ratio.

Macroscopically, a PS-BPLC is commonly treated as an optically isotropic medium.^{1,4} Based on this assumption, an excellent dark state (or very high CR) should be obtained when a BPLC cell is sandwiched between two crossed polarizers. But if this is true, then where does the light leakage come from? Some factors affecting the dark state light leakage have been investigated, such as Bragg reflection¹³ and light refraction on the edge of ITO (indium tin oxide) electrodes.¹⁴ Undoubtedly, these are important factors, but still another fundamental mechanism should be taken into consideration, which is optical rotatory power (ORP).¹⁵⁻¹⁸ According to Meiboom's model,¹⁹ BPLC is a three-dimensional structure consisting of double-twist cylinders whose diameter is around 100 nm. Inside each cylinder, LC molecules form double-twist structure. When the incident linearly polarized light traverses these cylinders, a small ORP could be accumulated depending on the cylinder's orientation. As a result, the polarization state of the outgoing light could be rotated by a small angle, which in turn leaks through the crossed polarizer and degrades the CR significantly.

In this Letter, we characterize the ORP of PS-BPLC samples with different Bragg reflection wavelengths (λ_B). Some double-twist cylinder orientations within a BPLC composite indeed cause the polarization axis of the transmitted beam to rotate and leak through the crossed polarizers. Rotating the analyzer in azimuthal direction to correct the ORP boosts the white light CR of the device by 3-5 \times . A modified De Vries equation based on a thin twist-nematic (TN) layer²⁰ is proposed to explain this phenomenon.

Our BPLC precursors consist of four ingredients: (1) nematic LC host (HTG135200-100), (2) right-handed chiral dopant (R5011); both are from HCCH China; (3) di-functional reactive monomer RM257 (Merck), and (4) mono-functional reactive monomer C12A (Sigma Aldrich). Detailed preparation process has been reported in Ref. 21. To obtain different Bragg reflection wavelengths, we varied the weight ratios of LC host and chiral dopant while fixing the monomer weight ratios at 6 wt. % RM257 and 4 wt. % C12A. The precursors were cured in the BP-I phase with a UV light ($\lambda \sim 365$ nm and intensity ~ 8 mW/cm²) for 10 min.

The experimental setup for characterizing the optical rotatory power of a BPLC cell is described as follows: Three laser wavelengths were used for measurement: R = 633 nm, G = 514 nm, and B = 457 nm. The transmission axis of the front linear polarizer was fixed, while the analyzer was crossed to the polarizer initially. The BPLC sample was sandwiched between the polarizers, and the light leakage measured. Without a sample, the extinction ratio of the crossed polarizers exceeds 10⁵:1.

We first investigated the BPLC cell with in-plane switching (IPS) electrodes. The electrode width/gap was 8 μ m/12 μ m, and cell gap d was 7.4 μ m. The upper half of Table I lists the measured transmittance (T_{\perp}) of this sample at the specified red-green-blue (RGB) wavelengths, when the analyzer was crossed. Surprisingly, T_{\perp} is still quite noticeable. But if we rotate the analyzer in azimuthal direction by a small angle α , a much smaller T'_{\perp} can be achieved for each wavelength, implying the outgoing light still keeps a fairly good linear polarization, but its polarization axis is rotated by α .

^{a)}Electronic mail: swu@ucf.edu

TABLE I. Polarization rotation effect: Comparison of IPS and VFS samples. T_{\perp} : Transmittance with analyzer crossed. T'_{\perp} : Transmittance with analyzer rotated by an angle α . Here, the positive α results from the employed right-handed chiral dopant.

λ (nm)	T_{\perp} (%)	α (deg)	α/d (deg/ μm)	T'_{\perp} (%)
IPS cell, $d = 7.4 \mu\text{m}$				
633	0.02	0.5	0.07	0.004
514	0.10	2.0	0.27	0.020
457	0.60	4.0	0.54	0.090
VFS cell, $d = 10 \mu\text{m}$				
633	0.02	0.5	0.05	0.004
514	0.20	2.5	0.25	0.020
457	1.0	5.5	0.55	0.080

This polarization rotation could originate from both BPLC material and light refraction at the edges of electrode; the latter has been reported in Ref. 14. To rule out the refraction effect and focus on the BPLC material property, we use the vertical-field switching (VFS) cell, which was made of two planar ITO glass substrates without polyimide layer.^{22,23} The cell gap was $d = 10 \mu\text{m}$. Similar to an IPS cell, we measure the light leakage of VFS sample. The results are included in the lower half of Table I. We find that crossed analyzer does not lead to the darkest state for either IPS or VFS cell. Rotating a small angle α can reduce the light leakage by 5-10 \times , depending on the wavelength. The VFS and IPS cells have similar α/d and T'_{\perp} values, indicating that these two cells have a similar optical rotatory property, resulting from the BPLC material property, not from the refraction on ITO electrode edge.

To focus on the material property, in the following experiments, we use VFS cells for all the measurements. Considering that outgoing light still keeps a good linear polarization, the polarization rotation angle caused by BPLC is the same as the analyzer rotation angle (α) from crossed position. ORP, $\varphi \equiv \alpha/d$, is defined as the polarization rotation angle divided by the cell gap. Unless otherwise mentioned, all measurements were conducted at room temperature (20 °C).

In experiment, we first investigate how the temperature affects ORP. We prepared a BPLC sample, designated as HTG-23, using the above mentioned recipes. Its Bragg reflection wavelength is $\lambda_B \sim 410 \text{ nm}$ and clearing point after UV curing is 78 °C. We measured its ORP at $\lambda = 514 \text{ nm}$ and 457 nm between 30 °C and 90 °C, and results are plotted in Figs. 1(a) and 1(b), respectively. In Fig. 1, circles represent the measured ORP values. The BPLC sample was placed on a rotary mount whose scale is 2° per division, so the precision of our data is $\pm 0.5^\circ$ in azimuthal angle. Therefore, the data shown in Fig. 1 appear stepwise. A positive ORP implies that polarization rotation is in the right-hand direction.

To understand the temperature dependent ORP data in Fig. 1, we measured the temperature dependent induced birefringence of the PS-BPLC, which in principle can be estimated from²⁴

$$\Delta n_s = \Delta n_0 C (1 - T/T'_c)^\beta, \quad (1)$$

where Δn_s is the saturated birefringence of Kerr-effect-induced isotropic-to-anisotropic transition in the BPLC,²⁵ Δn_0

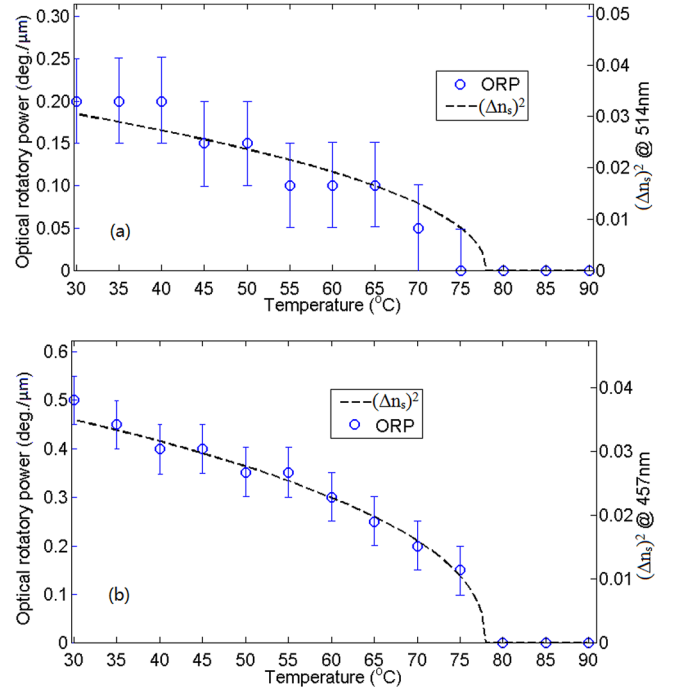


FIG. 1. Temperature dependent ORP (left) and $(\Delta n_s)^2$ (right) of HTG-23.

is the extrapolated birefringence of the LC host at $T = 0$, C is the LC host concentration (wt. %) in the composite, β is a material parameter, and T'_c is the clearing point of BPLC after UV curing. Using the measured data (not shown here), we obtained $\beta = 0.227$, and $\Delta n_0 = 0.296$, 0.321, and 0.347 for $\lambda = 633 \text{ nm}$, 514 nm, and 457 nm, respectively. Dashed lines in Fig. 1 represent the temperature dependent $(\Delta n_s)^2$. Semi-empirically, we found that ORP correlates with $(\Delta n_s)^2$ reasonably well

$$\varphi \propto (\Delta n_s)^2. \quad (2)$$

In total, we prepared 15 PS-BPLC samples with different λ_B 's, and measured their ORP at the specified RGB laser wavelengths. Results are plotted in Fig. 2. In Fig. 2, red open circles, green solid circles, and blue triangles represent the measured ORP of BPLC samples at $\lambda = 633 \text{ nm}$, 514 nm, and 457 nm, respectively, while red solid line, green dashed lines, and blue dotted lines are the corresponding fitting curves. The employed fitting equation will be discussed later. From Fig. 2, when λ_B increases towards the incident light wavelength λ , ORP increases rapidly. However, when λ_B gets closer to or longer than λ , ORP becomes difficult to measure because scattering dominates the transmitted light, and it is difficult to determine φ accurately.

The fast rising of ORP with λ_B can also be found in cholesteric liquid crystal as described by the De Vries equation.²⁶ De Vries equation has a term $(\lambda^2/\lambda_B^2 - 1)$ in the denominator, in which λ_B represents the Bragg reflection wavelength of a cholesteric LC. Therefore, it is reasonable to assume the equation of ORP in BPLC also has the same term in the denominator.

Finally, based on the above experimental results, we select the following equation to fit the ORP of our BPLC samples

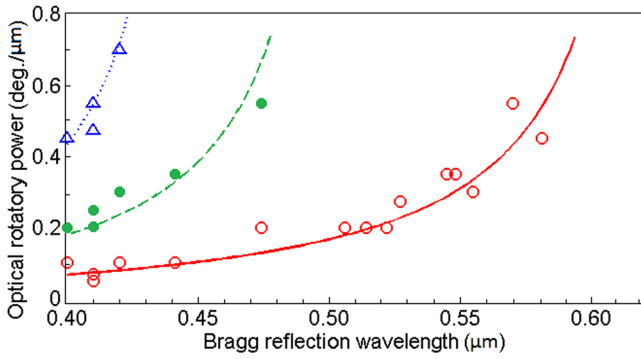


FIG. 2. Bragg reflection wavelength vs. optical rotatory power: red open circles are the measured ORP at $\lambda=633$ nm, green filled circles at $\lambda=514$ nm, and blue triangles at $\lambda=457$ nm. Lines are fitting curves using Eq. (3) with only one parameter $\varphi_0 = 3.12$ deg/ μm .

$$\varphi = \varphi_0 \frac{(\Delta n_s)^2}{\lambda^2 / \lambda_B^2 - 1}. \quad (3)$$

In Eq. (3), φ_0 is a fitting parameter, Δn_s is the saturated birefringence of BPLC, which is a function of wavelength and temperature, and λ_B is the Bragg reflection wavelength. We use Eq. (3) to fit the measured ORP data, as Fig. 2 shows. With only one fitting parameter ($\varphi_0 = 3.12$ deg/ μm), good agreement between experiment and Eq. (3) is obtained.

Figure 2 shows that the ORP of BPLC samples is in the 0.1°/ μm to 0.7°/ μm range. Since a typical BPLC cell gap is 5–10 μm , the analyzer could deviate by 0.5° to 7° from the perfectly crossed position. To see how this small deviation angle affects the device contrast ratio, we tested the BPLC samples HTG-23 again using the same experimental setup: First, we set the analyzer crossed to the polarizer. Then, we rotated the analyzer in azimuthal direction to minimize the light leakage for each wavelength. Result are shown in Fig. 3.

In Fig. 3, the horizontal axis shows the analyzer rotation angle (0° means the analyzer is crossed) and vertical axis represents the light leakage percentage (in logarithmic scale). Red open circles, green filled circles, and blue triangles are light leakage at $\lambda=633$ nm, 514 nm, and 457 nm,

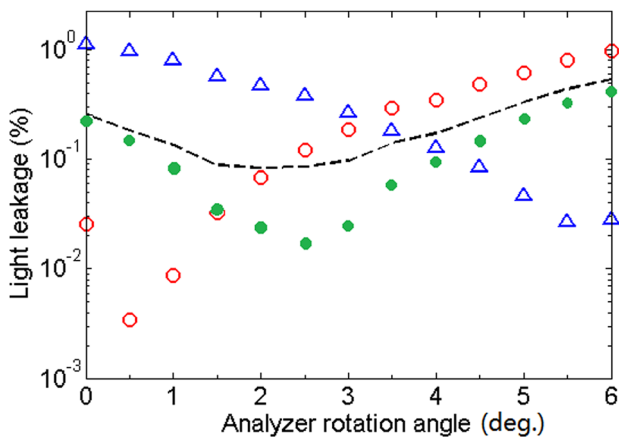


FIG. 3. Light leakage vs. analyzer rotation angle. Here, 0° means the analyzer is crossed with polarizer, and positive rotation angle represents rotation in right-hand direction. Red open circles are the measured light leakage at $\lambda=633$ nm, green filled circles at $\lambda=514$ nm, and blue triangles at $\lambda=457$ nm. Dashed lines are the overall leakage of white light, including 30% red, 60% green, and 10% blue lights.

respectively. From Fig. 3, the dark state light leakage can be reduced by $\sim 10\times$ for a given wavelength by adjusting the analyzer’s angle. However, each wavelength has its own optimal analyzer angle. For LCDs, a white backlight is usually comprised of 60% green, 30% red, and 10% blue spectral contents. We take these ratios into account and calculate the overall white light leakage as the black dashed lines shown in Fig. 3. When the analyzer is crossed, white light leakage is $\sim 0.25\%$, corresponding to CR $\sim 320:1$, assuming the bright state transmittance is 80% for a typical IPS cell. If we rotate the analyzer by $\sim 2^\circ$, the white light leakage drops to $\sim 0.08\%$, and the CR is boosted to 1000:1. Moreover, based on Eq. (3), if we shift λ_B from 410 nm to 350 nm (this is a common practice for a clear BPLC), the overall leakage would decrease noticeably, and the white light contrast ratio would exceed 3000:1.

Next, we try to explain the observed optical rotatory power by a thin TN model. It is known that in BP-I phase, the LC molecules are arranged in double-twist cylinders, as sketched in Fig. 4, and these cylinders are stacked to form body-centered cubic (BCC) structure. Let us assume the incident light is in the positive z direction in Fig. 4, the optical activity of each cylinder is illustrated too. Due to the random alignment of BCC domains, the incident light could propagate along any direction into the cylinders. But for the simplicity of discussion, we focus on the basic configurations, when the incident wave vector is either parallel or perpendicular to the cylinder’s axis. On the left side of Fig. 4, the incident light propagates along the cylinder’s axis. Because the LC molecules in the cylinder are aligned equally in all directions, the cylinder appears optically isotropic, which does not affect the polarization state of the incident light. However, for the other two cylinders in Fig. 4, the light propagation directions are perpendicular to their axis. Therefore, as the light traverses the cylinder, it will interact with the 90° twisted LC directors. This twisted alignment affects the outgoing polarization of the light. Generally speaking, the outgoing light will be elliptically polarized, with the long axis of this ellipse rotated by a certain angle θ away from incident polarization direction, as shown in Fig. 4. This phenomenon is similar to the case when the light passing through a very thin TN cell. Thus, we simulate the optical activity of a TN cell by Jones matrix and see if we can find analogy between TN and BPLC.

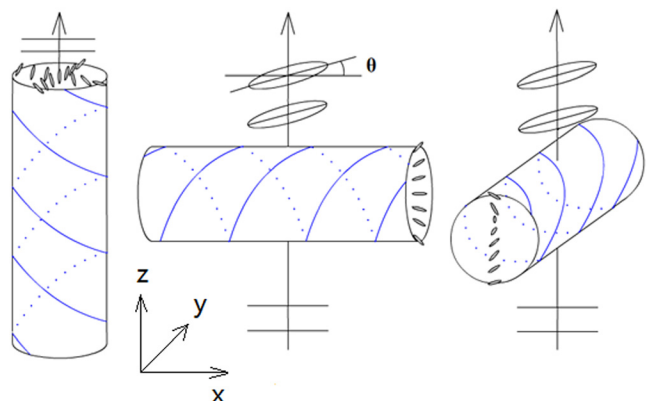


FIG. 4. LC director configuration in BP-I phase: Double-twist cylinders.

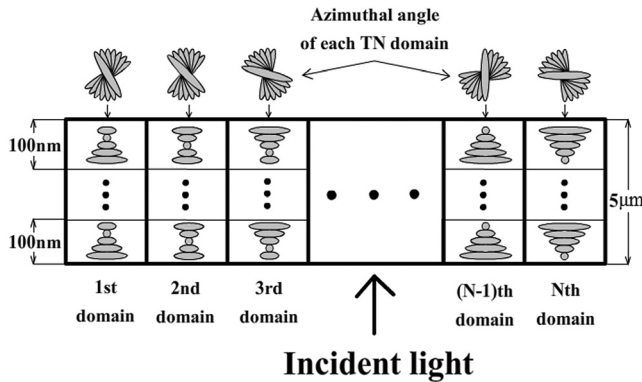


FIG. 5. The multi-domain multi-layer TN cell structure used in the simulation. Upper part: top view, and lower part: cross-section view.

Considering that in a VFS cell, there are multiple micro-domains of BPLC, aligning in different directions. Besides, the BCC structure of BPLC has multiple layers of double-twist cylinders stacked inside each domain. Therefore, to imitate the optical activity of BPLC precisely, we use a multi-domain, multi-layer TN LC cell model, as shown in Fig. 5. We divide a 5- μm -thick LC cell into N ($N > 100$) domains. Each aligned in a random azimuthal angle, and divided into multiple layers. Each layer is a 100-nm-thick TN cell with 90° twist angle in right hand direction. The LC birefringence is 0.2, and the wavelength is 550 nm.

We simulate the polarization of the light passing through each TN domain and then take the average of all domains. Results are depicted in Fig. 6. Here, horizontal and vertical coordinates represent the amplitudes of light in x and y directions. Black dotted lines show the incident light, linearly polarized in x direction. The outgoing light (the solid blue line) is elliptically polarized, but the eccentricity of this ellipse is close to unity, so it looks like a linear polarization with polarization direction rotated by 4.5° . So the ORP in the thin TN model is defined as the rotation angle of the ellipse's long axis divided by the cell gap. Based on simulation result, this ORP is described by

$$\varphi = \varphi_0 \frac{(\Delta n)^2}{\lambda^2 / \lambda_B^2}, \quad (4)$$

where φ_0 is a constant, Δn is the LC birefringence, and λ_B is the Bragg reflection wavelength of this cell, determined by the refractive index and the thickness of each TN layer. Note that Eq. (4) is quite similar to Eq. (3) except for the denominator. Actually, Eq. (3) is reduced to Eq. (4) when $\lambda_B \ll \lambda$. The physical meaning of this approximation is when the Bragg reflection wavelength is much shorter than the incident wavelength, Bragg reflection is negligible. Under this approximation, the optical activity of BPLC could be explained by this thin TN model.

In conclusion, we have investigated the polarization rotation of polymer-stabilized BPLCs. The effects of birefringence, Bragg reflection wavelength, and incident light wavelength on the ORP of BPLC are evaluated. It is shown that by correcting the ORP, the device contrast ratio can be improved by more than $3\times$. A thin TN model is proposed to explain the polarization rotation phenomenon. Simulation

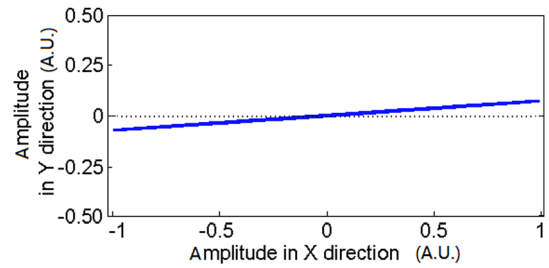


FIG. 6. Polarization state change of the light passing through a multi-domain multi-layer TN cell: black dotted lines show the incident polarization state. Blue solid line shows the simulated outgoing polarization state.

result based on this model is found to be an approximation of experimental results when $\lambda_B \ll \lambda$.

The authors are indebted to Jie Sun, Jin Yan, and Yuan Chen for useful discussion and AU Optronics (Taiwan) for financial support.

- ¹H. Kikuchi, M. Yokota, Y. Hisakado, H. Yang, and T. Kajiyama, *Nature Mater.* **1**, 64 (2002).
- ²S. W. Choi, S. I. Yamamoto, Y. Haseba, H. Higuchi, and H. Kikuchi, *Appl. Phys. Lett.* **92**, 043119 (2008).
- ³Z. Ge, S. Gauza, M. Jiao, H. Xianyu, and S. T. Wu, *Appl. Phys. Lett.* **94**, 101104 (2009).
- ⁴J. Yan, L. Rao, M. Jiao, Y. Li, H. C. Cheng, and S. T. Wu, *J. Mater. Chem.* **21**, 7870 (2011).
- ⁵H. Lee, H. J. Park, O. J. Kwon, S. J. Yun, J. H. Park, S. Hong, and S. T. Shin, *SID Int. Symp. Digest Tech. Papers* **42**, 121 (2011).
- ⁶K. M. Chen, S. Gauza, H. Xianyu, and S. T. Wu, *J. Display Technol.* **6**, 49 (2010).
- ⁷Y. Chen, J. Yan, J. Sun, S. T. Wu, X. Liang, S. H. Liu, P. J. Hsieh, K. L. Cheng, and J. W. Shiu, *Appl. Phys. Lett.* **99**, 201105 (2011).
- ⁸L. Rao, Z. Ge, S. T. Wu, and S. H. Lee, *Appl. Phys. Lett.* **95**, 231101 (2009).
- ⁹L. Rao, J. Yan, S. T. Wu, S. Yamamoto, and Y. Haseba, *Appl. Phys. Lett.* **98**, 081109 (2011).
- ¹⁰M. Wittek, N. Tanaka, D. Wilkes, M. Bremer, D. Pauluth, J. Canisius, A. Yeh, R. Yan, K. Skjonnemand, and M. Klasen-Memmer, *SID Int. Symp. Digest Tech. Papers* **43**, 25 (2012).
- ¹¹K. M. Chen, S. Gauza, H. Xianyu, and S. T. Wu, *J. Display Technol.* **6**, 318 (2010).
- ¹²L. Rao, J. Yan, S. T. Wu, Y. H. Chiu, H. Y. Chen, C. C. Liang, C. M. Wu, P. J. Hsieh, S. H. Liu, and K. L. Cheng, *J. Display Technol.* **7**, 627 (2011).
- ¹³Y. Hirakata, D. Kubota, A. Yamashita, T. Ishitani, T. Nishi, H. Miyake, H. Miyairi, J. Koyama, S. Yamazaki, T. Cho, and M. Sakakura, *J. Soc. Info. Display* **20**, 38 (2012).
- ¹⁴S. Yoon, G.-H. Yang, P. Nayek, H. Jeong, S.-H. Lee, S.-H. Hong, H.-J. Lee, and S.-T. Shin, *J. Phys. D: Appl. Phys.* **45**, 105304 (2012).
- ¹⁵D. Bensimon, E. Domany, and S. Shtrikman, *Phys. Rev. A* **28**, 427 (1983).
- ¹⁶V. A. Belyakov and V. E. Dmitrienko, *Sov. Phys. Usp.* **28**, 535 (1985).
- ¹⁷Z. Kutnjak, C. W. Garland, C. G. Schatz, P. J. Collings, C. J. Booth, and J. W. Goodby, *Phys. Rev. E* **53**, 4955 (1996).
- ¹⁸B.-Y. Zhang, F.-B. Meng, and Y.-H. Cong, *Opt. Express* **15**, 10175 (2007).
- ¹⁹S. Meiboom, J. P. Sethna, W. P. Anderson, and W. F. Brinkman, *Phys. Rev. Lett.* **46**, 1216 (1981).
- ²⁰M. Schadt and W. Helfrich, *Appl. Phys. Lett.* **18**, 127 (1971).
- ²¹J. Yan and S. T. Wu, *Opt. Mater. Express* **1**, 1527 (2011).
- ²²H. C. Cheng, J. Yan, T. Ishinabe, and S. T. Wu, *Appl. Phys. Lett.* **98**, 261102 (2011).
- ²³J. Yan, Y. Chen, S. T. Wu, and X. Song, *J. Display Technol.* **9**, 24 (2013).
- ²⁴S. T. Wu and C. S. Wu, *Phys. Rev. A* **42**, 2219 (1990).
- ²⁵J. Yan, H. C. Cheng, S. Gauza, Y. Li, M. Jiao, L. Rao, and S. T. Wu, *Appl. Phys. Lett.* **96**, 071105 (2010).
- ²⁶H. Baessler, T. M. Laronge, and M. M. Labes, *J. Chem. Phys.* **51**, 3213 (1969).